Magneto-optical Kerr effect in short-period CdTe/MnTe superlattices

M. Pohlt, W. Herbst, and H. Pascher
Experimentalphysik I, Universität Bayreuth, D-95440 Bayreuth, Germany

W. Faschinger* and G. Bauer
Institut Für Halbleiterphysik, Universität Linz, A-4040 Linz, Austria

(Received 8 August 1997; revised manuscript received 3 November 1997)

Magneto-optical Kerr effect (MOKE) studies of biaxially strained $(CdTe)_n/(MnTe)_n$ superlattices gives evidence of an antiferromagnetic ordering as well as of paramagnetic behavior (bulk MnTe is an antiferromagnet with $T_N \approx 70$ K). With increasing n, paramagnetic behavior becomes dominant in the MOKE signals, apparently caused by the lack of spin ordering at the (CdTe)/(MnTe) interfaces for wider CdTe wells. Apart from the magnetic properties, the MOKE signals also yield information on the electronic interband transitions involving heavy-hole and electron subbands, centered in the CdTe quantum wells. [S0163-1829(98)06416-9]

I. INTRODUCTION

Magnetic semiconductor quantum structures have found increasing interest in recent years, because strong spin-spin interactions lead to interesting magneto-optical and magnetotransport phenomena.[1–4] Among those semiconductors, structures based on II-VI compounds have particularly been studied quite intensively. However, while the electronic and magnetic properties of $CdTe/Cd_{1-x}Mn_xTe$, $ZnSe/Zn_{1-x}Mn_xSe$, or $ZnSe/Zn_{1-x}Fe_xSe$ quantum-well and superlattice structures have been investigated quite thoroughly,[5–9] the amount of information on the superlattices consisting of binary compounds like CdTe/MnTe or ZnSe/MnSe is still much more sparse.

In the following we will concentrate on the CdTe/MnTe system as a model quantum structure system for a diamagnetic/antiferromagnetic layer sequence. It is well known that for proper growth conditions MnTe can be obtained in its metastable cubic zinc-blende modification (fcc lattice), if it is grown epitaxially on fcc substrates. The energy gap of CdTe bulk material is 1.606 eV,[10] and the gap of MnTe epilayers was precisely measured by luminescence ($E_g = 3.3$ eV) (Ref. 11) and optical reflectance experiments on thick MnTe films ($E_g \approx 3.2$ eV).[12] It has been established that $CdTe/Cd_{1-x}Mn_xTe$ superlattices are of type I,[13] and it is supposed that CdTe/MnTe superlattices are of type I as well.

The magnetic properties of zinc-blende MnTe were investigated by Ando, Takahashi, and Okuda who measured the magnetic susceptibility and magnetic circular dichroism.[14] The magnetic structure was ascertained by neutron diffraction.[15] It turned out that cubic MnTe is a close realization of a Heisenberg fcc antiferromagnet with dominating nearest-neighbor (NN) exchange interactions. The localized spins of the Mn^{2+} ions are antiferromagnetically ordered in (100) planes, as recently shown for cubic MnTe epilayers by neutron diffraction experiments (AFM-III structure).[15] Perpendicularly to these sheets, antiferromagnetic NN-interaction is partially frustrated. The resulting strong ground-state degeneracy can be partially removed by lattice distortions in superlattices. Indeed, in CdTe/MnTe superlattices, incommensurate helical antiferromagnetic domains were found.[16] The phase transition between antiferromagnetic and paramagnetic phases has been observed at approximately 70 K, with some variations depending on strain in a homogeneous MnTe epilayer, and at about 85 K in MnTe/ZnTe superlattices.[15]

It has been reported that the magnetic behavior may change if the magnetic layer thickness approaches the two-dimensional limit. Sawicki *et al.* investigated a series of $(CdTe)_n/(Cd_{0.5}Mn_{0.5}Te)_m$ superlattices with constant $n = 16$ and m varying from 5 to 20.[17] In superconducting quantum interference device magnetization experiments, a reduction of the spin-glass freezing temperature with decreasing thickness of the magnetic barrier was measured. But a transition to a spin-glass state was observed in every investigated sample.

In $Cd_{0.5}Mn_{0.5}Te/Cd_{0.89}Mn_{0.11}Te$ superlattices, the Raman line connected with the magnon excitations at low temperature was not observed, although it is present in bulk samples of $Cd_{0.5}Mn_{0.5}Te$. In the superlattices, only Raman paramagnetic lines were detected.[18]

A transition from antiferromagnetic to paramagnetic behavior in very thin films was also observed by Awschalom *et al.*[19] Measurements of the magnetic susceptibility in thick epitaxial layers of $Cd_{1-x}Mn_xTe$ at low temperatures show a well-defined cusp in magnetic susceptibility vs temperature associated with the spin-glass transition similar to that in bulk material. However, very thin epilayers of $Cd_{1-x}Mn_xTe$ with comparable Mn content x exhibit a monotonic paramagnetic behavior, which is explained by a frustration of the antiferromagnetic coupling in thin layers, because the number of nearest neighbors is reduced.[20,21] Additionally, for a discussion of paramagnetic behavior in superlattices, one should have in mind interface effects like intermixing and roughness as discussed for the $CdTe/Cd_{1-x}Mn_xTe$ system, e.g., by Gaj and co-workers.[22,23] High-resolution transmission electron microscopy on MnTe layers showed that there is an increased interface broadening for the growth of CdTe on MnTe with increasing MnTe layer thickness.[23,24] The reduction of magnetic nearest neighbors reduces the antiferromagnetic spin ordering, particularly in the first MnTe atomic layers close to the CdTe interfaces.

Direct observation of the spin ordering in CdTe/MnTe superlattices is obtained in neutron-diffraction experiments. Indeed, not only conclusive evidence of antiferromagnetic ordering was found, but also strong indications of magnetic interactions between the MnTe layers across the CdTe layers. The diffraction peaks for the antiferromagnetic interaction are accompanied by satellite peaks, and the helical spin ordering depends sensitively on the number of MnTe and CdTe monolayers.[25,26] This magnetic coupling across the CdTe layers also stabilizes the antiferromagnetic ordering in the first MnTe atomic layers, and compensates for its above-discussed reduction the more effectively the thinner the CdTe layers are.

Recently, polaronic effects in CdTe/MnTe structures were suggested to occur as well,[27] and Quazzaz *et al.* showed that the electron paramagnetic resonance spectra of isolated Mn^{2+} ions, which diffused into the CdTe layers of CdTe/MnTe multiple-quantum-well structures with constituent layer thicknesses of about 12 nm, yield a direct measure of the strain.

In the present work, we describe an optical method for the investigation of the evaluation of magnetic interactions in $(CdTe)_n/(MnTe)_n$ superlattices with increasing n. Since the GaAs substrate is not transparent in the spectral region of interest around 2 eV, instead of transmission experiments (Faraday effect), magneto-optical experiments using the reflected light were carried out. We show that magneto-optical Kerr effect (MOKE) experiments, which probe the interaction of the wave function of the carriers confined in the CdTe wells with the magnetic species, give relevant information on the spin ordering.

II. THEORETICAL BACKGROUND

The magneto-optical Kerr effect denotes the rotation of the polarization plane of linearly polarized light, when it is reflected from matter in a magnetic field, which is aligned parallel to the propagation of the incident light. The rotation angle Θ depends on the spin splitting of the optical transitions. In the spectral range used in our experiments, interband transitions dominate. The different phase shifts occurring at reflection for the two circular components of the reflected light lead to the rotation of the linearly polarized wave.[29]

The spin splittings of the conduction and valence bands contain information about the magnetization of the sample. Whenever the probability to find a charge carrier at the lattice location of a Mn^{2+} ion is finite, exchange interaction between the spin of the localized electrons and the mobile carriers will contribute to the spin splitting of the band electrons and holes. Therefore, the spin levels of the mobile carriers do not only split in the external magnetic field (Zeeman effect), but in addition they split proportionally to the magnetization.

The index of refraction for the two circular polarizations σ^+ and σ^- of radiation with photon energy E can be described near an excitonic transition in a magnetic field by a single-oscillator model according to

$$\tilde{n}_{\pm}^{2} = \varepsilon^{\pm}(E,B) = \varepsilon_{\infty} + \frac{F_0}{E_0^{\pm}(B) - E - \frac{1}{2} i\Gamma^{\pm}(B)}. \quad (1)$$

$E_0^{\pm}(B)$ are the excitonic transition energies for left- and right-hand circularly polarized light, F_0 denotes a constant proportional to the oscillator strength, $\Gamma^{\pm}(B)$ is a phenomenological damping constant, and ε_{∞} is the high-frequency dielectric constant. In the limit of small damping Eq. (1) corresponds to Eq. (2) of Ref. 28. In (semi)magnetic materials, the excitonic transition energies for left- and right-hand circularly polarized light contain a contribution proportional to the magnetization $M(B,T)$ of the sample:[30]

$$\Delta E = E_0^{+}(B) - E_0^{-}(B) = \Delta E_0(B) + \Delta E[M(B,T)]. \quad (2)$$

Due to Eq. (1), the magneto-optical effects show strong signatures in the frequency dependence of the angle of rotation at fixed B at the interband transition energies $E_0^{\pm}(B)$, which are a function of the magnetization of the sample [see Eq. (2)]. Thus the dependence of the MOKE signal on magnetic field or temperature yields information on the magnetization of the sample.

In the present samples, the splitting of the excitonic transition energies of left- and right-hand circularly polarized light is much smaller than the linewidth of the excitonic transitions. Therefore the rotation angle depends linearly on the splitting of these transitions.

Since in our experiments the light can penetrate the superlattice and the buffer layer and is partially reflected by the various interfaces, one cannot observe pure MOKE (reflection from surface). Multiple reflections combined with the Faraday effect of the traversing light lead to interference fringes in the Kerr angle of the thin samples.

Knowing the indices of refraction for all layers and both circular polarizations, the phase shifts occurring with reflections at all the interfaces as well as with penetration through the individual layers are obtained. Using the matrix formalism as described by Nies and Kessler,[31] the total magneto-optical effect in transmission as well as in reflection can be calculated.

The line shapes of the resonances due to interband transitions strongly depend on the relative energetic positions of excitonic resonances and interference maxima arising from the above-mentioned multiple reflections. Figure 1 shows examples for calculated line shapes occurring for the same layer thicknesses but slightly different resonance energies. It is obvious that strong changes in the line shape occur. A careful line-shape analysis must be performed to find the correct resonance positions as well as amplitudes of the signatures.

In the CdTe/MnTe superlattices the strongest signatures are due to interband transitions between heavy-hole and electron subbands in the CdTe wells. These transition energies can be extracted after a line-shape analysis directly from the measured spectra. The wave functions of the involved states penetrate into the MnTe barriers. Thus information on the magnetic properties, particularly of the first MnTe layers close to the CdTe/MnTe interfaces is obtained.

III. EXPERIMENTAL DETAILS

All samples were grown on [001]-oriented GaAs with a combined method of molecular-beam epitaxy and atomic layer epitaxy.[32] A relaxed buffer layer of ZnTe ($\approx$1 μm

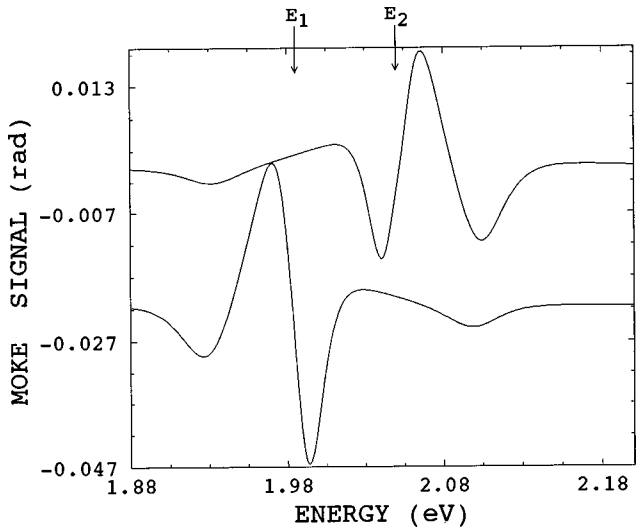

FIG. 1. Theoretical MOKE line shapes calculated regarding Fabry-Perot-like interferences in the multilayer structure. Excitonic transitions at $E_1=1.985$ eV (lower trace) and $E_2=2.05$ eV (upper trace). The geometry of the sample is equal in both cases.

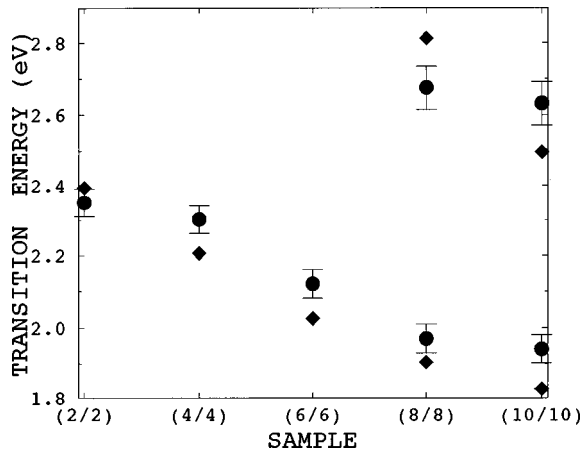

FIG. 2. Measured optical transition energies at 6.81 T in the samples: full circles. Kronig-Penney calculation ($B=0$): diamonds.

thick) ensures that the superlattices also grow in [001] direction.[32] For the growth of the CdTe and MnTe layers of the superlattice, a method as described in Ref. 32 was chosen: the CdTe layers were grown by atomic layer epitaxy in the 0.5-ML/cycle modus. The MnTe layers were grown in the conventional molecular-beam-epitaxy modus, but monitoring the fluxes with a quadrupole mass spectrometer with a feedback loop for the shutter control. As previously shown, this growth method yields comparatively well-defined short-period superlattices with much less intermixing than those obtained by conventional molecular-beam epitaxy (for further details, see Ref. 32). All samples contain nominally equal thicknesses of CdTe and fcc MnTe of 2, 4, 6, 8, and 10 ML each. The CdTe and MnTe layers in these short-period superlattices, with the number of double layers ranging from about 70 to 300, grow approximately strain symmetrized. High-resolution x-ray-diffraction data already show superlattice satellite peaks for samples with the smallest number of monolayers. The simulations of the x-ray data using dynamical diffraction theory revealed that the maximum deviation of the MnTe layer thicknesses from their nominal values in this series of samples is less than 10%.[32,33]

The detection of very small rotation angles of the polarization direction can be achieved by using differential methods. One method uses two orthogonally polarized components of the linearly polarized wave separated behind the sample by a polarizing beam splitter. They are focused onto two detectors. If the light is linearly polarized along the 45° direction with respect to the axis of the beam splitter, the difference between the intensities of the two components vanishes. A rotation of the polarization plane then can be determined from the difference of the two intensities.[34]

We have improved this experimental setup by using a photoelastic modulator switching the polarization of the incident beam by 90° at a frequency of 114.4 kHz. Behind the sample an analyzer is adjusted to 45° with respect to the incident polarizations. In addition, the light was chopped at about 500 Hz. One detector is then sufficient for both the detection of the difference of the intensities of the orthogonally polarized waves and the measurement of the total intensity (using two lock-in amplifiers). If there is no ellipticity of the light reflected from the sample, one can calculate the angle of rotation from both signals. For small angles and small ellipticities, the signal depends linearly on the angle and only quadratically on the ellipticity, so it is rather insensitive to ellipticity.

The experiments were carried out using a superconducting magnet equipped with a variable-temperature insert. The windows of the cryostat are exposed to the strong magnetic field. Owing to Faraday effect, they induce a rotation of the polarization plane of about 15° ($B=6.8$ T, $\lambda=500$ nm). The Kerr rotation due to the sample is of the order 0.01°. The best way to separate the sample rotation from the high window background is to measure the MOKE signal as it depends on the wavelength. The variation of the window rotation with the wavelength of the light is small compared to the amplitudes of the signatures due to interband transitions within the samples. Therefore, in two independent measurements the rotation due to the windows and the sample can be separated.

IV. RESULTS AND DISCUSSION

A. Interband transition energies

Figure 2 shows the experimentally determined interband transition energies in high magnetic fields of 6.8 T (full circles), as well as the approximation with a Kronig-Penney calculation (diamonds). In contrast to photoluminescence experiments, with the magneto-optical Kerr effect, higher subband transitions in the superlattice can also be detected. They are also depicted in Fig. 2.

For the calculation it was assumed that 80% of the energy-gap difference occurs as conduction-band offset as it is the case in $CdTe/Cd_{1-x}Mn_xTe$ structures.[35] The effective masses of MnTe were calculated according to the extrapolation formula also given in Ref. 35. Regarding the uncertainties in band offsets and effective masses, there is a satisfactory agreement between the calculations and the experimental data. But, despite the fact that the calculation neglects the exciton binding energy, the calculated transition

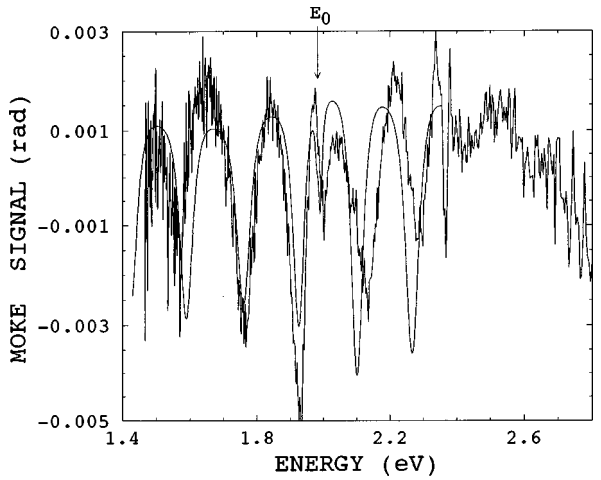

FIG. 3. MOKE spectrum of the sample with 8-ML CdTe and MnTe ($B=0$ T, $T=1.8$ K). Line without noise: Simulation assuming $|n_+ - n_-| = 2.5\times10^{-4}$ in the epilayers, probably due to strain.

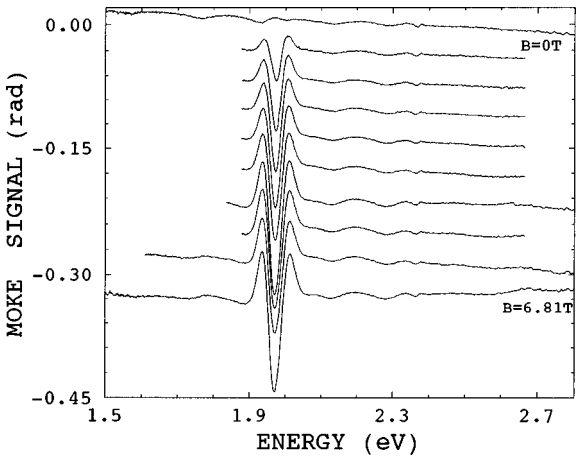

FIG. 4. MOKE spectra of the sample with 8-ML CdTe and MnTe at $T=1.8$ K. Uppermost trace: $B=0$; lowest trace: $B=6.8$ T; equidistant B steps (vertical offsets for clarity). Note the evolution of the E_0 signature at about 1.98 eV, resulting from the lowest interband transition.

energies in most cases are too low. However, the limited accuracy of a Kronig-Penney calculation and the uncertainties of the MnTe effective masses do not allow one to calculate band offsets from the remaining discrepancy between calculated and observed transition energies.

B. Magnetic properties

At zero magnetic field, no magneto-optical dichroism is expected. However, the experimental recording displayed in Fig. 3 clearly shows small but existing MOKE signals with an interference structure. This cannot be explained as a consequence of any magnetic ordering, because it still exists at a temperature of 100 K, far above the transition temperature reported in literature for MnTe.

An experimental result as shown in Fig. 3 can be caused either by rotation of the plane of polarization or by ellipticity of the reflected light. The latter is less probable, because the detection method is rather insensitive to ellipticity. Assuming that a rotation of the polarization is caused by strain in the epilayers [$d_{SL}\approx0.4$ μm, $d_{ZnTe}=1$ μm (Ref. 32)], one can approximately explain the experimental data (see calculated line without noise in Fig. 3). In a phenomenological model calculation we described the observed rotation by a splitting of the indices of refraction for left- and right-hand circularly polarized light to be 2.5×10^{-4}. The periodicity of the interference fringes indicates that the dominating Fabry-Perot resonator is built by the superlattice and the buffer together.

There is an additional signature marked by ''E_0'' in Fig. 3. This transition can be reproduced in the theoretical simulation [see Eq. (1)] assuming an exciton in the CdTe layers with $E_0=1.982$ eV, $F_0=2$ meV, and $\Gamma=7.3$ meV. The regular structure stops abruptly at about 2.38 eV, the energy gap of the ZnTe buffer. This proves our above mentioned assumption that the effective resonator includes the buffer layer.

Figure 4 shows MOKE measurements as a function of photon energy for various (equidistant) magnetic fields. There exists a structure at about 1.98 eV which drastically grows in amplitude with increasing magnetic field. The growth in amplitude of the interference fringes is just about a factor of 2. This indicates that most of the effect on MOKE, owing to the spin splitting, occurs within the exciton linewidth. The amplitude $\Delta\Theta$ of the interband signature contains information about the magnetization of the sample [see Eq. (2)]. The fact that the line shape does not change drastically with increasing magnetic field demonstrates that the splitting of the excitonic interband transitions is indeed much smaller than the excitonic linewidth.

The analogous curves for the other samples were measured as well. The magnetic-field dependence of the amplitudes of the resonance signatures at 1.8 K is plotted in Fig. 5. In the sample with 2 ML of each material, the amplitude depends linearly on the magnetic field. With increasing layer thicknesses one observes an enhanced Brillouin function like bending of the corresponding curves, which is a clear indi-

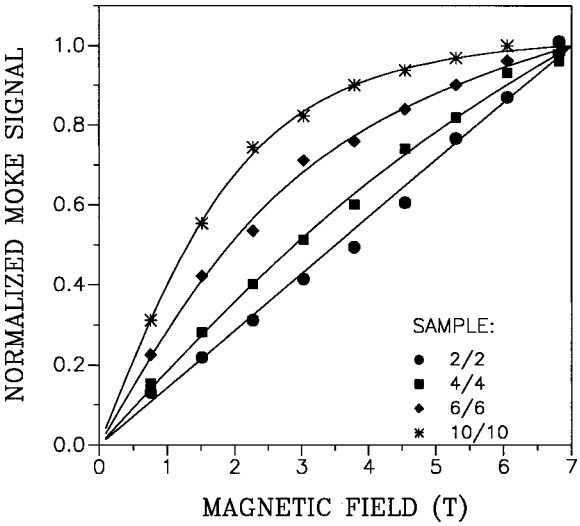

FIG. 5. Magnetic-field dependence of the amplitudes of the E_0 signatures in the MOKE spectra ($T=1.8$ K) normalized to the value at 7 T for all samples. The solid lines are fitted Brillouin function [see text: Eq. (3)].

TABLE I. Fit results of Eq. (3) on experimental data according to Fig. 5. The estimated accuracy of the parameters is ±10%.

Sample	10/10	6/6	4/4	2/2
$m(t/\mathrm{T})$	0	0.032	0.075	0.143
b	1.04	0.83	0.58	0
T_0 (K)	2.0	3.15	6.45	
b/m (T)	$\rightarrow\infty$	26.0	7.7	0

cation for paramagnetic behavior. To quantify the paramagnetic contribution to the total rotation, we have fitted the function

$$\Delta\Theta = m\left[B + \frac{b}{m} B_J\left(\frac{g_l J \mu_B B}{k(T+T_0)}\right)\right] \tag{3}$$

to the experimental data, where m and b are free parameters. g_l is the g factor of the localized Mn^{2+} electrons ($g_l = 2$). B_J is a modified Brillouin function.[36] $J = \frac{5}{2}$ accounts for the Mn magnetic moment, and T_0 describes a small antiferromagnetic coupling of the more or less isolated Mn ions, responsible for the paramagnetic behavior.[36] b/m is the relative weight of the Brillouin function B_J. This parameter shows a rapid increase with increasing layer thickness (see Table I), indicating an increasing paramagnetic behavior of the localized Mn^{2+} electrons in the interface regions of the superlattice where the mobile carriers, which cause the MOKE signal, can be found. In Table I we also list the fit results for T_0. There is a slight increase of T_0, with decreasing layer thickness observed. It should be noted that the experimental data cannot be described by a modified Brillouin function without the term linear in B. Such a model works well with samples with larger periods, but fails for samples with smaller periods.

The existence of disordered Mn^{2+} ions, especially near the interfaces between MnTe and CdTe, is in agreement with resonance coherent Raman experiments, where a Raman paramagnetic peak was observed in addition to the Raman antiferromagnetic resonance, e.g., in the sample with 8 ML.[37]

The linear part of the magnetic-field dependence of the rotation angles can be caused either by the normal Zeeman splitting of the mobile carriers in the diamagnetic CdTe quantum wells or the antiferromagnetic part of the susceptibility at low temperature. However, in diluted magnetic $Cd_{1-x}Mn_xTe$ with higher Mn concentration, a nearly linear increase of the magnetization with the magnetic field has also been observed.[38] However, the *temperature dependence* of the rotation angles is different for these effects. The Zeeman splitting of the spin levels is expected to be constant with temperature, while the magnetization of an antiferromagnet shows a cusp at the transition temperature between antiferromagnetic and paramagnetic phases.

Figure 6 shows the temperature dependence of the amplitudes of the interband signatures in the Kerr spectra for the samples with 2, 4, 6, and 10 ML in a high magnetic field of 6.8 T. For the sample with the widest period (10 ML), only paramagnetic behavior in the region of the charge carriers is observed. The solid line is a fitted Brillouin function ($T_0 = 0$, since temperatures are high compared to the results in Table I). In the sample with the smallest period (2+2 ML), however, no paramagnetic behavior at all is present at low temperature. The maximum of the Kerr amplitude and thus of the magnetization indicates a transition temperature of about 75 K. The temperature dependence of the MOKE amplitude (and of the magnetization deduced from it) is in sharp contrast to the one observed for a diluted magnetic material. Using just optical data, one can compare the MOKE data with the spin splitting of free electrons (e.g., photoexcited in undoped material), which also has a contribution proportional to the magnetization. We measured this spin splitting in a bulk $Cd_{0.6}Mn_{0.4}Te$ sample by coherent Raman scattering, and found that it decreases according to a Curie-Weiss law for $T \geqslant 20$ K and is constant for $T < 20$ K.[39] This behavior is in contrast to the uppermost curve in Fig. 6. This comparison between the magnetic behavior of the CdTe/MnTe (2/2 ML) sample and the $Cd_{0.6}Mn_{0.4}Te$ bulk material is clear experimental evidence that the MOKE signal in the 2/2 sample is not dominated by randomly oriented spins in an intermixed region at the interfaces, but rather that, with this magneto-optical method, we observe an antiferromagnetic ordering of the Mn spins across the thin CdTe layers, due to interlayer coupling. The latter results in a suppression of any paramagnetic signal in the thinnest superlattice sample. Furthermore, we note that the temperature dependence of the magnetization deduced from Fig. 6 for the 2/2 sample is different from published data for bulk like MnTe.[14,17] We apparently observe a behavior well known for the susceptibility in parallel fields ($\chi_\parallel$) of an antiferromagnet. The latter fact demonstrates the orientation of the Mn spins due to strain.

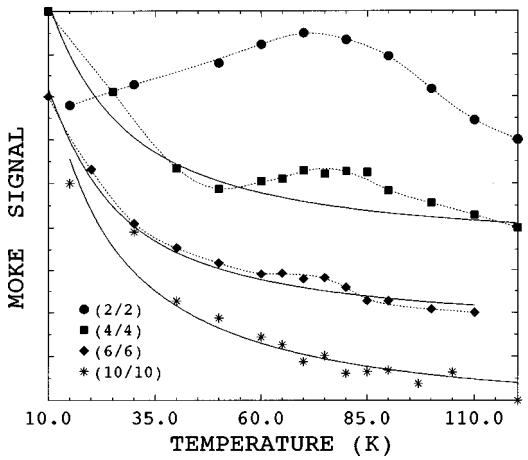

FIG. 6. Temperature dependence of the amplitudes of the E_0 signatures in the MOKE spectra ($B = 6.8$ T) for different samples. The solid lines are fitted Brillouin functions (see text). Dotted lines are a guide for the eye.

The other two samples exhibit a gradual transition between the two extreme cases observed with the 10/10 and 2/2 samples, respectively. The solid lines again are fitted Brillouin functions with the experimental data between 60 and 90 K not taken into account. However, we note that there is a systematic deviation of the experimental points from the Brillouin functions in the range of the phase-transition temperature for the 4/4 and 6/6 samples. This indicates that the

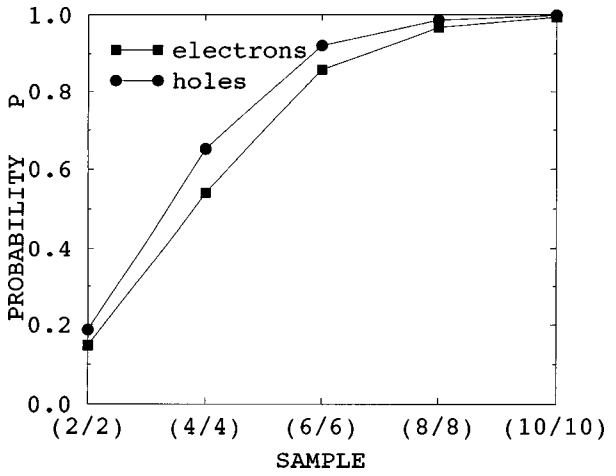

FIG. 7. Normalized difference of probabilities to find electrons and holes, respectively, at the CdTe/MnTe interfaces and in the MnTe-barrier center: $P=(|\psi_{\text{interface}}|^2-|\psi_{\text{center}}|^2)/(|\psi_{\text{interface}}|^2+|\psi_{\text{center}}|^2)$ (Kronig-Penney model) vs number of MnTe and CdTe monolayers.

wave functions of the mobile electrons and holes overlap with two regimes in the MnTe layers, i.e., paramagnetic and antiferromagnetically ordered regions.

For an understanding of these observations, it has to be considered that the experiment probes the magnetization due to the Mn ions located within the regions with nonvanishing expectation probabilities of mobile carriers. In Fig. 7, we plot the normalized difference of the square of the wave functions at the interfaces and in the center of the MnTe layers (for the calculations, we used a Kronig-Penney model as described in Sec. IV A). It is seen that with the 10/10 sample the probability to find an electron in the center of MnTe is practically zero. Consequently the MOKE signal yields information on the magnetization of the Mn ions at the interface which is mainly paramagnetic (see Sec. I).

In order to check this assumption, magnetization measurements with the 10/10 sample have been performed.[40] A quantitative analysis of these data shows that 11% of the Mn ions contained in the sample, that means one ML per superlattice period, are not antiferromagnetically ordered. The Curie-Weiss temperature, fitted to the paramagnetic contribution to the magnetization arising from these ions, is 4.5 K, in fairly good agreement with the value of T_0 resulting from the MOKE data (see Table I). In contrast to MOKE, magnetization probes the entire sample, regardless of the expectation probabilities to find electrons in the respective layers. Thus, in the magnetization experiment, the antiferromagnetic phase transition is also observed at a temperature of about 50 K.

With decreasing layer thickness, the wave functions penetrate more and more into MnTe, and in the 2/2 sample less than a 20% difference between the expectation probabilities at the center and the interface occurs. Accordingly, antiferromagnetic coupling within the MnTe layers increasingly shows up from the 10/10 to the 2/2 samples in the MOKE data. But, more than that, with decreasing CdTe thickness the interface regions of the MnTe also become increasingly ordered due to the interlayer coupling, resulting in a complete suppression of paramagnetism in the 2/2 sample.

We are well aware of the fact that the molecular-beam-epitaxy-grown samples exhibit monolayer fluctuations. At a first glance these fluctuations should change the magnetic properties of CdTe/MnTe superlattices considerably. However, as the neutron diffraction data have shown, the antiferromagnetic interactions through sufficiently thin diamagnetic CdTe layers are so strong as to orient effectively all spins of the $3d$ electrons of the Mn ions, whether these reside in completely filled or partially filled atomic Mn layers at the interfaces. However, with increasing CdTe layer thickness, these interactions weaken, and the frustrated antiferromagnetism evolves into a paramagnetic behavior in the partially filled layers.

Microscopic information on the interface roughness could be obtained from x-ray standing-wave studies, which are known to be sensitive to the position and the disorder of very thin layers (less than a monolayer to several monolayers; see, e.g., Ref. 41). However, such experiments on multilayers are not easily interpreted, and quantitative analysis is usually restricted to single buried layers. On the other hand, for magnetization and neutron diffraction measurements, CdTe/MnTe multilayers are required by the signal-to-noise ratio.

V. CONCLUSION

We have shown that the magneto-optical Kerr effect yields information on both the magnetic behavior and interband transition energies. As far as the magnetic behavior is concerned, one has to bear in mind that, with MOKE interactions of the carrier wave functions with the magnetic ions in the barriers are probed. From neutron-scattering data it is well established that, in all the samples investigated, antiferromagnetic ordering is present. Whether in the MOKE signal this antiferromagnetic behavior shows up or not depends sensitively on the penetration of the wave function into the barriers. With increasing numbers of MnTe monolayers, antiferromagnetic behavior is less and less pronounced. Furthermore, it is evident that the antiferromagnetic interlayer coupling across the CdTe layers is stronger the thinner the wells are. Consequently, the $n=2$ sample exhibits strong antiferromagnetic features in the MOKE signal, which are absent for the $n=10$ sample. The decreasing antiferromagnetic interlayer coupling apparently strongly influences the spin order at the CdTe/MnTe interfaces. For the $n=10$ sample in this interface region, the antiferromagnetic ordering is absent, and a strong paramagnetic signal results. In the samples between these two extreme cases, a coexistence of ordered and disordered areas occurs, and consequently both antiferromagnetic and paramagnetic behaviors are present in the MOKE signal, clearly seen in the temperature dependence of the amplitudes.

ACKNOWLEDGMENTS

The project was financially supported by the Deutsche Forschungsgemeinschaft (DFG), Bonn and the Fonds zur Förderung der wissenschaftlichen Forschung (FWF), Vienna. We wish to thank R. Rupprecht and H. Sitter for helpful discussions.

*Present address: Phys. Institut, Universität Würzburg, D-97074 Würzburg, Germany.

[1] For reviews on diluted magnetic semiconductors, see, e.g., J. K. Furdyna, J. Appl. Phys. **64**, R29 (1988); T. Dietl, in *Handbook on Semiconductors*, edited by T. S. Moss (North-Holland, Amsterdam, 1994), Vol. 3b, p. 1251.

[2] D. D. Awschalom and N. Samarth, in *Optics of Semiconductor Nanostructures*, edited by F. Henneberger, S. Schmitt-Rink, and E. O. Goebel (Akademie Verlag, Berlin, 1993), and references therein.

[3] I. P. Smorchkova, N. Samarth, J. M. Kikkawa, and D. D. Awschalom, Phys. Rev. Lett. **78**, 3571 (1997).

[4] A. Haury, A. Wasiela, A. Arnoult, J. Cibert, S. Tatarenko, T. Dietl, and Y. Merle d'Aubigne, Phys. Rev. Lett. **79**, 511 (1997).

[5] N. Dai, H. Lou, F. C. Zhang, N. Samarth, M. Dobrowolska, and J. K. Furdyna, Phys. Rev. Lett. **67**, 3824 (1991).

[6] W. C. Chou, A. Petrou, J. Warnock, and B. T. Jonker, Phys. Rev. Lett. **67**, 3820 (1991).

[7] X. Liu, A. Petrou, J. Warnock, B. T. Jonker, G. A. Prinz, and J. J. Krebs, Phys. Rev. Lett. **63**, 2280 (1989).

[8] D. D. Awschalom, M. R. Freeman, N. Samarth, H. Lou, and J. K. Furdyna, Phys. Rev. Lett. **66**, 1212 (1991).

[9] G. Mackh, W. Ossau, A. Waag, and G. Landwehr, Phys. Rev. B **54**, R5227 (1996).

[10] *Semiconductors*, edited by K. H. Hellwege and O. Madelong, Landolt-Börnstein, New Series, Group III (Springer-Verlag, Berlin, 1987), Vol. 22a.

[11] R. Rupprecht (private communication).

[12] S. M. Durbin, J. Han, O. Sungki, M. Kobayashi, D. R. Menke, R. L. Gunshor, Q. Fu, N. Pelekanos, A. V. Nurmikko, D. Li, J. Gonsalves, and N. Otsuka, Appl. Phys. Lett. **55**, 2087 (1989).

[13] E. L. Ivchenko, A. V. Kavokin, V. P. Kochershko, G. R. Posina, I. N. Uraltsev, D. R. Yakovlev, R. N. Bicknell-Tassius, A. Waag, and G. Landwehr, Phys. Rev. B **46**, 7713 (1992).

[14] K. Ando, K. Takahashi, and T. Okuda, J. Magn. Magn. Mater. **104–107**, 993 (1992).

[15] T. M. Giebultowicz, P. Klosowski, N. Samarth, H. Luo, J. K. Furdyna, and J. J. Rhyne, Phys. Rev. B **48**, 12 817 (1993).

[16] T. M. Giebultowicz, W. Faschinger, V. Nunez, P. Klosowski, G. Bauer, H. Sitter, and J. K. Furdyna, J. Cryst. Growth **138**, 877 (1994).

[17] M. Sawicki, S. Kolesnik, T. Wojtowicz, G. Karczewski, E. Janik, M. Kutrowski, A. Zarzewsik, T. Dietl, and J. Kossut, Superlattices Microstruct. **15**, 475 (1994).

[18] S. Venugopalan, L. A. Kolodziejski, R. L. Gunshor, and A. K. Ramdas, Appl. Phys. Lett. **45**, 974 (1984).

[19] D. D. Awschalom, J. M. Hong, J. L. Chang, and G. Grinstein, Phys. Rev. Lett. **59**, 1733 (1987).

[20] W. J. Ossau and B. Kuhn-Heinrich, Physica B **184**, 422 (1993).

[21] J. Cibert, W. Grieshaber, J. A. Gaj, Y. Merle d'Aubigné, and A. Wasiela, Mater. Sci. Forum **182–184**, 567 (1995).

[22] J. A. Gaj, C. Bodin-Deshayes, P. Peyla, J. Cibert, G. Feuillet, Y. Merle d'Aubigné, R. Romestain, and A. Wasiela, in *21st International Conference on the Physics of Semiconductors, Beijing, China, 10–14 Aug. 1992*, edited by Ping Jiang and Hou-Zhi Zheng (World Scientific, Singapore, 1992), Vol. 2, p. 1936.

[23] J. A. Gaj, W. Grieshaber, C. Bodin-Deshayes, J. Cibert, G. Feuillet, Y. Merle d'Aubigné, and A. Wasiela, Phys. Rev. B **50**, 5512 (1994).

[24] P. H. Jouneau, A. Tardot, G. Feuillet, H. Mariette, and J. Cibert, Inst. Phys. Conf. Ser. **134**, 329 (1993).

[25] V. Nunez, T. M. Giebultowicz, W. Faschinger, G. Bauer, H. Sitter, and J. K. Furdyna, J. Magn. Magn. Mater. **140–144**, 633 (1995).

[26] V. Nunez, T. M. Giebultowicz, W. Faschinger, G. Bauer, H. Sitter, and J. K. Furdyna, in *22nd International Conference on the Physics of Semiconductors, Vancouver, BC, Canada, 15–19 Aug. 1994*, edited by D. J. Lockwood (World Scientific, Singapore, 1995), Vol. 3, p. 2521.

[27] Z. Wilamowski, W. Jantsch, G. Hendorfer, H. Krenn, J. Sperl, and W. Faschinger, Mater. Sci. Forum **182–184**, 553 (1995).

[28] M. Quazzaz, G. Yang, S. H. Lin, L. Montes, H. Luo, and J. K. Furdyna, Solid State Commun. **96**, 405 (1995).

[29] I. M. Boswarva, R. E. Howard, and A. B. Lidiard, Proc. R. Soc. London, Ser. A **269**, 125 (1962).

[30] D. U. Bartholomew, J. K. Furdyna, and A. K. Ramdas, Phys. Rev. B **34**, 6943 (1986).

[31] R. Nies and F. R. Kessler, Phys. Status Solidi A **111**, 639 (1989).

[32] E. Abramof, W. Faschinger, H. Sitter, and A. Pesek, J. Cryst. Growth **135**, 447 (1994).

[33] M. de Naurois, J. Stangl, W. Faschinger, G. Bauer, and S. Ferreira, J. Appl. Phys. **81**, 6120 (1997).

[34] M. Kohl and D. D. Awshalom, Phys. Rev. B **43**, 2431 (1991).

[35] A. Chitta and Gilmar E. Marques, Semicond. Sci. Technol. **3**, 564 (1987).

[36] J. A. Gaj, R. Planel, and G. Fishman, Solid State Commun. **29**, 435 (1979).

[37] R. Rupprecht, H. Pascher, W. Faschinger, H. Sitter, and G. Bauer, J. Cryst. Growth (to be published).

[38] J. P. Lascaray, M. C. D. Duruelle, and D. Coquillat, Phys. Rev. B **35**, 675 (1987).

[39] R. Rupprecht, B. Müller, H. Pascher, I. Miotkowski, and A. K. Ramdas (unpublished).

[40] H. Krenn (private communication).

[41] J. C. Boulliard, B. Capelle, S. Gualandris, A. Lifchitz, J. Cibert, and S. Tatarenko, J. Appl. Phys. **81**, 1173 (1997).